

Supplementary material

Designing Solution-Processed Thermally Activated Delayed Fluorescence Emitters via Introducing Bulky Steric Hindrance Groups for Pure Red OLEDs

Table of contents

Supplementary Note 1: Methods	S1
Supplementary Note 2: Materials synthesis	S3
Supplementary Note 3: NMR and HRMS spectra.....	S5
Supplementary Note 4: Supplementary figures	S10
Supplementary References.....	S10

Supplementary Note 1: Methods

S 1.1 Characterization

The nuclear magnetic resonance (NMR) spectra were obtained using a Bruker AVANCE III 400 spectrometer (400 MHz) or a Bruker AVANCE III 500 spectrometer (500 MHz). ¹H-NMR and ¹³C-NMR were measured with TMS as internal standard. ¹H-NMR spectra data are reported as chemical shift, relative integral, multiplicity (s=singlet, d=doublet, m=multiplet), coupling constant (J in Hz) and assignment.

Molecular masses were determined by a MALDI-FTICR-MS with anhydrous dichloromethane as the matrix.

Ultraviolet-visible (UV-Vis) absorption spectra were recorded on a Hitachi U-2910 spectrophotometer in air atmosphere.

Room and ultra-low temperature (77 K) and photoluminescence (PL) spectra were recorded on Hitachi F-7000 fluorescence spectrophotometer. The energy gap (ΔE_{ST}) between the lowest singlet (S₁) and triplet excited states (T₁) were determined from the difference values of the onset positions of fluorescence and phosphorescence spectra.

Fluorescence decay of doped films (x wt% doped in 5 wt% poly(N-vinylcarbazole) (PVK) and 100-x wt% tris(4-carbazoyl-9-ylphenyl) amine (TCTA)) were recorded in vacuum on a FS-5 spectrometer from Edinburgh Instruments Limited with picosecond pulsed diode laser emitting at 300 nm. Temperature-dependent fluorescence decay from 77 K to 300 K were also measured with the support of Oxford variable temperature accessories. The ΔE_{ST} of three emitters were calculated using the Arrhenius equation by using the following equations:

$$\ln k_{RISC} = -\frac{\Delta E_{ST}}{RT} + c \#(S0)$$

The photo luminance quantum yields (PLQYs) of the blended films were measured on FS-5 with an integrating sphere ($\varphi = 150$ mm). The quantum efficiencies and rate constants were determined using the following equations according to the literatures¹:

$$k_{PF} = \frac{\Phi_{PF}}{\tau_{PF}} \#(S1)$$

$$k_{DF} = \frac{\Phi_{DF}}{\tau_{DF}} \#(S2)$$

$$k_{ISC} = \frac{\Phi_{PF}}{\Phi_{PF} + \Phi_{DF}} k_{PF} \#(S3)$$

$$k_{RISC} = \frac{k_{PF} k_{DF} \Phi_{DF}}{k_{ISC} \Phi_{PF}} \#(S4)$$

$$k_{PF} = k_r^S + k_{nr}^S + k_{ISC}^S \quad \#(S5)$$

$$k_r^S = \eta_{PF} \cdot k_{PF} \quad \#(S6)$$

$$k_{nr}^S = k_{PF} - k_r^S - k_{ISC}^S \quad \#(S7)$$

The PLQYs of the materials in vacuum can be converted by integrating the steady state spectrum, and the PLQY in air. The equation is as follows:

$$PLQY_{vac} = \frac{I_{vac}}{I_{air}} PLQY_{air} \quad \#(S8)$$

In which, I_{vac} and I_{air} is the integrate of the steady state spectrum in vacuum and air atmospheres, respectively.

Cyclic voltammetry (CV) was carried out in nitrogen-purged acetonitrile at room temperature with a CHI voltametric analyzer. Tetrabutylammonium hexafluorophosphate (TBAPF6 0.1 M) was used as the supporting electrolyte. The conventional three-electrode configuration consists of a glassy carbon working electrode, a platinum wire auxiliary electrode, and an Ag/AgNO₃ pseudo-reference electrode with ferrocenium-ferrocene (Fc⁺/Fc) as the external standard. Cyclic voltammograms were obtained at scan rate of 100 mV s⁻¹. The onset potential was determined from the intersection of two tangents drawn at the rising and background current of the cyclic voltammogram. The highest occupied molecular orbital (HOMO) and lowest unoccupied molecular orbital (LUMO) energy levels were calculated according to the external reference ferroceneredox couple in dichloromethane by using the following formulas²:

$$E_{HOMO} = - \left(E_{\left(\begin{smallmatrix} onset,ox \\ vx \end{smallmatrix} \frac{Fc^+}{Fc} \right)} + 4.8 \right) \quad \#(S9)$$

$$E_{HOMO} = - \left(E_{\left(\begin{smallmatrix} onset,red \\ vx \end{smallmatrix} \frac{Fc^+}{Fc} \right)} + 4.8 \right) \quad \#(S10)$$

The morphologies of the pure films and blended films (3 wt% tBuInPz-DQ and 5 wt% tBuInPz-SP doped in 5 wt% PVK and 93 wt% TCTA) coated on the quartz substrate were measured using atomic force microscopy (Agilent Technologies 5500) under tapping mode.

Differential scanning calorimetry (DSC) was conducted using a TA Q2000 differential scanning calorimeter under a nitrogen atmosphere. The temperature was increased from 30 °C to 300 °C at a rate of 20 °C/min, followed by cooling to -10 °C at the same rate, and then heating to 280 °C at a rate of 10 °C/min. The glass transition temperature (T_g) was determined from the exothermic step observed during the second heating cycle. Thermogravimetric analysis (TGA) was performed with a METTLER TOLEDO TGA/DSC 1/1100SF instrument at a heating rate of 20 °C min⁻¹ from 30 to 800 °C under nitrogen atmosphere.

S 1.2 Molecular simulation

Density functional theory (DFT) calculation was performed by Gaussian 09 in the B3LYP mode with a 6-31G (d, p) basis set in the ground state. According to the optimized results, HOMO and LUMO levels can be obtained. The excited states energy levels and the energy properties in the excited states were determined using Gaussian 09 with a PBE1PBE/DFE2SVP basis in time dependent (TD) mode. To boost the calculation precision of the singlet and triplet energy levels, the number of calculated states was set to 10. The natural transition orbital (NTO) analysis was performed using Multiwfn 3.6 based on Gaussian output results.^{4,5} The distributions of hole and electron can be found from the NTO results and the dominate nature, charge transfer (CT) or local excited state (LE), can be found out by the overlap integral of main contribution orbits.

Supplementary Note 2: Materials synthesis

The donor molecule tBulnPz was synthesized according to the reported literature, and all raw materials can be obtained commercially.

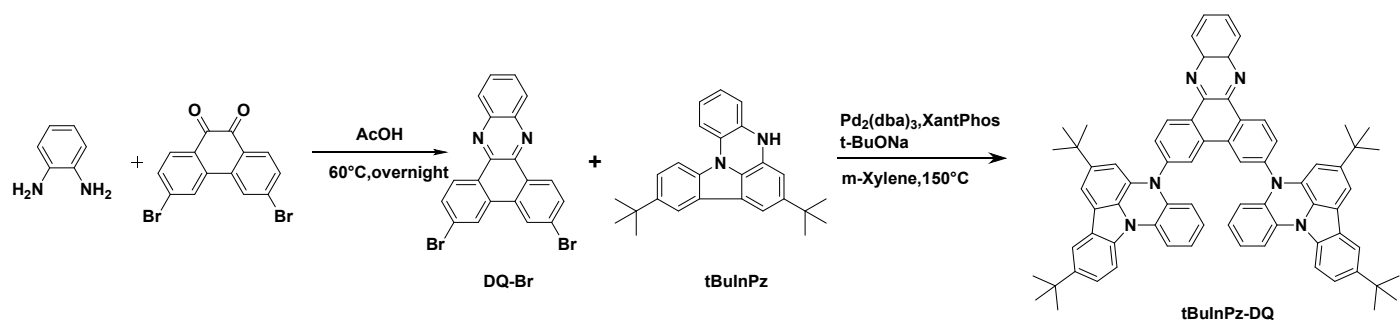


Figure S1. Synthesis routes of tBulnPz-DQ.

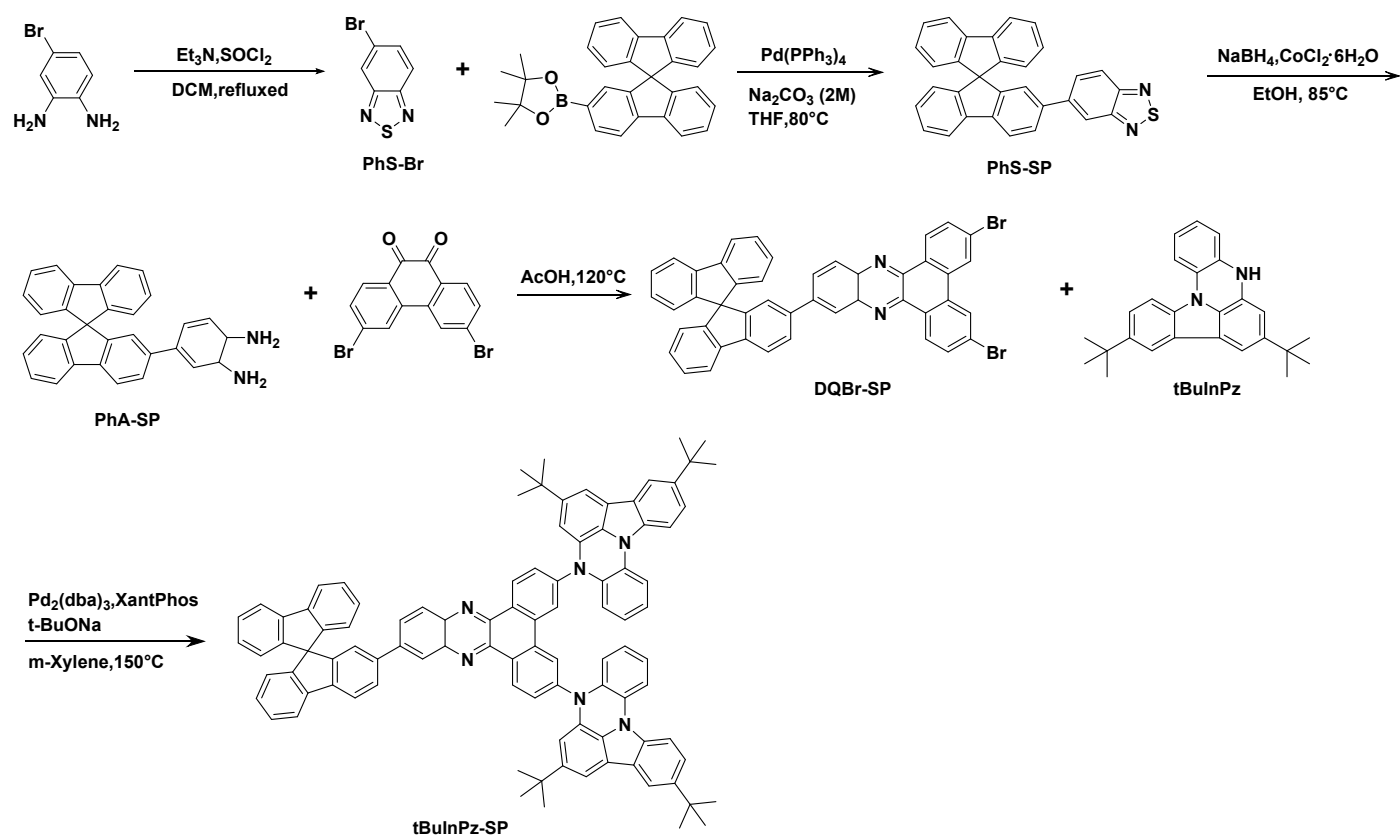


Figure S2. Synthesis routes of tBulnPz-SP.

Synthesis of DQ-Br

Aniline (1.08 g, 10.0 mmol) and 3,6-dibromoanthracene (3.64 g, 10.0 mmol) were placed in a two-necked flask and dissolved in 20 mL of glacial acetic acid. The reaction mixture was heated at 120°C for 9 hours. After cooling to room temperature, the reaction mixture was poured into 100 mL of water and filtered under reduced pressure using a Büchner funnel. The organic phase was washed three times with 20 mL of dichloromethane and then three times with 20 mL of methanol. After each washing step, the solid residue was obtained by vacuum filtration. The resulting solid residue was dried under vacuum to yield a yellow solid powder. Yield: 92%. ¹H-NMR (400 MHz, chloroform-d) δ (ppm): 9.29 (d, J = 8.5 Hz, 2H), 8.63 (d, J = 1.3 Hz, 2H), 8.33 (s, 2H), 7.89 (d, J = 6.8 Hz, 4H).

Synthesis of tBulnPz-DQ

tBulnPz (0.36 g, 1.0 mmol) and DQ-Br (218 mg, 0.5 mmol) were dissolved in 10 mL of xylene. To this mixture, bis(dibenzylideneacetone)palladium (10 mg, 0.01 mmol), Xantphos (23 mg, 0.04 mmol), and tBuONa (96 mg, 1.0 mmol) were added, and the reaction was carried out at 150 °C for 8 hours. The reaction mixture was washed with saturated sodium chloride solution, and then extracted with dichloromethane. The organic layer was dried over anhydrous magnesium sulfate, filtered, and the solvent was removed by rotary evaporation. The orange solid powder was purified by column chromatography. Yield: 75%. ¹H-NMR (600 MHz, d₈-tetrahydrofuran) δ (ppm): 9.77 (d, J = 8.5 Hz, 2H), 9.00 (d, J = 2.1 Hz, 2H), 8.41 (dd, J = 6.4 Hz, 3.4 Hz, 2H), 8.03 (d, J = 2.0 Hz, 2H), 7.97 (dd, J = 6.5 Hz, 3.5 Hz, 2H), 7.94 (d, J = 2.1 Hz, 1H), 7.93 (s, 2H), 7.91 (s, 1H), 7.66 (dd, J = 8.1 Hz, 1.5 Hz, 2H), 7.52 (dd, J = 8.8 Hz, 5.1 Hz, 2H), 7.22 (d, 1.4 Hz, 2H), 6.74 (td, 7.3 Hz, 1.3 Hz, 2H), 6.57 (td, 8.3 Hz, 1.3 Hz, 2H), 6.18 (dd, J = 8.0 Hz, 1.3 Hz, 2H), 5.93 (d, J = 1.3 Hz, 2H), 1.43 (s, 18H), 1.11 (s, 18H). ¹³C-NMR (151 MHz, d₈-tetrahydrofuran) δ (ppm): 146.96, 143.83, 143.54, 143.17, 138.38, 135.81, 135.61, 134.89, 131.99, 131.50, 131.45, 131.43, 130.70, 130.56, 130.50, 127.69, 126.38, 124.51, 122.53, 122.50, 117.91, 115.77, 114.90, 113.04, 113.07, 107.66, 104.85, 35.59, 35.44, 32.37, 32.16. MALDI-MS: m/z [M⁺] calcd for C₇₂H₆₆N₆ 1015.5309 found 1015.5319.

Synthesis of PhS-Br

Under argon atmosphere, 4-bromobenzene-1,2-diamine (5.58 g, 30.0 mmol) was placed in a three-necked flask and dissolved in 50 mL of anhydrous dichloromethane. To this solution, 18 mL of triethylamine was slowly added. Separately, 7 mL of sulfonyl chloride was dissolved in 10 mL of anhydrous dichloromethane and added dropwise to the three-necked flask under ice bath conditions. The reaction mixture was then heated to reflux for 5 hours. After the reaction, methanol was added to quench the reaction, and the solvent was removed under reduced pressure. 100 mL of water was added, and the pH was adjusted to 1 by dropwise addition of concentrated hydrochloric acid. The organic phase was extracted three times with dichloromethane, and the combined organic phases were washed, dried, and concentrated under reduced pressure. The resulting orange solid powder was purified by column chromatography. Yield: 80%. ¹H-NMR (400 MHz, chloroform-d) δ (ppm): 8.22 (d, J = 1.2 Hz, 1H), 7.88 (d, J = 9.3 Hz, 1H), 7.67 (dd, J = 9.3 Hz, 1.8 Hz, 1H).

Synthesis of PhS-SP

PhS-Br (1.07 g, 5 mmol), 2-(9,9'-spirobi[fluoren]-2-yl)-4,4,5,5-tetramethyl-1,3,2-dioxaborolane (2.21 g, 5 mmol), and Pd(PPh₃)₄ (175 mg, 0.15 mmol) were dissolved in 75 mL of tetrahydrofuran. To this solution, 15 mL of 2 M sodium carbonate solution was added, and the reaction mixture was stirred at 80 °C for 24 hours. After the reaction, the solvent was removed under reduced pressure. The reaction mixture was washed with saturated sodium chloride solution and then extracted with dichloromethane. The organic layer was dried over anhydrous magnesium sulfate, filtered, and the solvent was removed by rotary evaporation. The resulting orange solid powder was purified by column chromatography. Yield: 75%. ¹H-NMR (400 MHz, chloroform-d) δ (ppm): 8.00 (d, J = 1.0 Hz, 1H), 7.97 (d, J = 10.8 Hz, 1H), 7.90 (dd, J = 18.8 Hz, 8.3 Hz, 4H), 7.73 (ddd, J = 9.2, 5.9, 1.8 Hz, 1H), 7.40 (tdd, J = 7.6, 4.9, 1.1 Hz, 3H), 7.14 (qd, J = 7.6, 1.1 Hz, 3H), 7.05 (d, J = 1.7 Hz, 1H), 6.78 (dd, J = 10.8 Hz, 7.6 Hz, 3H).

Synthesis of DQBr-SP

PhS-SP (450 mg, 1 mmol), NaBH₄ (230 mg, 6 mmol), and cobalt (II) chloride hexahydrate (8 mg, 0.03 mmol) were dissolved in 50 mL of anhydrous ethanol. The reaction mixture was stirred at 85 °C for 6 hours. After cooling the reaction mixture to room temperature, the resulting solution was filtered under reduced pressure. The solvent was removed under reduced pressure, and the residue was vacuum-dried to obtain a white solid mixture (PhA-SP) weighing 400 mg. The PhA-SP was then placed in a two-neck flask, and 3,6-dibromoanthracene (364 mg, 1 mmol) was added. The mixture was dissolved in 20 mL of glacial acetic acid and refluxed at 120 °C for 9 hours. After cooling the reaction mixture to room temperature, it was poured into 100 mL of water and filtered under reduced pressure using a Büchner funnel. The organic phase obtained after filtration was washed three times with 20 mL of dichloromethane and then three times with 20 mL of methanol. After each washing step, the solid residue was collected by vacuum filtration. The final solid residue obtained after vacuum drying was a yellow powder. Yield: 51%. ¹H-NMR (400 MHz, chloroform-d) δ (ppm): 9.23 (t, J = 8.6 Hz, 2H), 8.61 (d, J = 1.7 Hz,

2H), 8.35 (s, 1H), 8.26 (d, J = 8.8 Hz, 1H), 8.05 (d, J = 6.5 Hz, 2H), 7.94 (q, J = 6.0, 5.3 Hz, 4H), 7.87 (dd, J = 9.4, 4.7 Hz, 2H), 7.44 (td, J = 7.6, 1.2 Hz, 3H), 7.26 (s, 1H), 7.18 (td, J=7.2, 2.6 Hz, 3H), 6.85 (d, J = 7.6 Hz, 2H), 6.80 (d, J = 7.5 Hz, 1H).

Synthesis of tBulnPz-SP

tBulnPz (0.36 g, 1.0 mmol) and DQBr-SP (376 mg, 0.5 mmol) were dissolved in 10 mL of xylene. To this mixture, bis (dibenzylideneacetone)palladium (10 mg, 0.01 mmol), Xantphos (23 mg, 0.04 mmol), and tBuONa (96 mg, 1.0 mmol) were added, and the reaction was carried out at 150 °C for 8 hours. The reaction mixture was washed with saturated sodium chloride solution, and then extracted with dichloromethane. The organic layer was dried over anhydrous magnesium sulfate, filtered, and the solvent was removed by rotary evaporation. The orange solid powder was purified by column chromatography. Yield: 73%. ¹H-NMR (500 MHz, d8-tetrahydrofuran) δ (ppm): 9.70 (dd, J = 8.6, 3.9 Hz, 2H), 8.97 (s, 2H), 8.46 (d, J = 2.2 Hz, 1H), 8.34 (d, J = 9.0 Hz, 1H), 8.16 (ddd, J = 11.7, 6.0, 2.2 Hz, 2H), 8.07 (dd, J = 8.0, 1.8 Hz, 1H), 8.02 (q, J = 0.5 Hz, 2H), 8.00 (s, 1H), 7.96 (d, J = 7.6 Hz, 2H), 7.93 (d, J = 2.9 Hz, 1H), 7.91 (t, J = 2.6 Hz, 2H), 7.89 (t, J = 2.4 Hz, 1H), 7.88 (d, J = 2.1 Hz, 1H), 7.65 (d, J = 8.1 Hz, 2H), 7.53 (d, J = 2.3 Hz, 1H), 7.51 (t, J = 2.6 Hz, 1H), 7.39 (t, J = 7.6 Hz, 3H), 7.31 (s, 1H), 7.21 (d, J = 5.3 Hz, 2H), 7.14 (t, J = 7.5 Hz, 3H), 6.79 (d, J = 7.5 Hz, 2H), 6.74 (dd, J = 7.8, 3.2 Hz, 2H), 6.71 (d, J = 7.0 Hz, 1H), 6.55 (td, J = 8.0, 3.2 Hz, 2H), 6.16 (t, J = 7.3 Hz, 2H), 5.90 (d, J = 4.8 Hz, 2H), 1.43 (d, J = 2.8 Hz, 18H), 1.10 (d, J = 2.8 Hz, 18H). ¹³C-NMR (151 MHz, d8-tetrahydrofuran) δ (ppm): 151.18, 150.62, 149.74, 146.93, 143.80, 143.78, 143.68, 143.59, 143.50, 143.15, 142.99, 142.92, 142.88, 142.31, 140.35, 138.36, 138.34, 135.76, 135.67, 135.59, 134.88, 134.85, 131.91, 131.88, 131.47, 131.43, 131.40, 131.30, 130.66, 130.50, 130.43, 129.17, 128.89, 128.56, 127.64, 127.13, 126.36, 125.00, 124.52, 124.41, 123.86, 122.49, 121.85, 121.40, 121.18, 117.91, 115.77, 115.74, 114.88, 113.05, 108.26, 104.85, 35.59, 32.37, 32.15. MALDI-MS: m/z [M⁺] calcd for C₉₇H₈₀N₆ 1328.6444 found 1328.6444.

Supplementary Note 3: NMR spectra

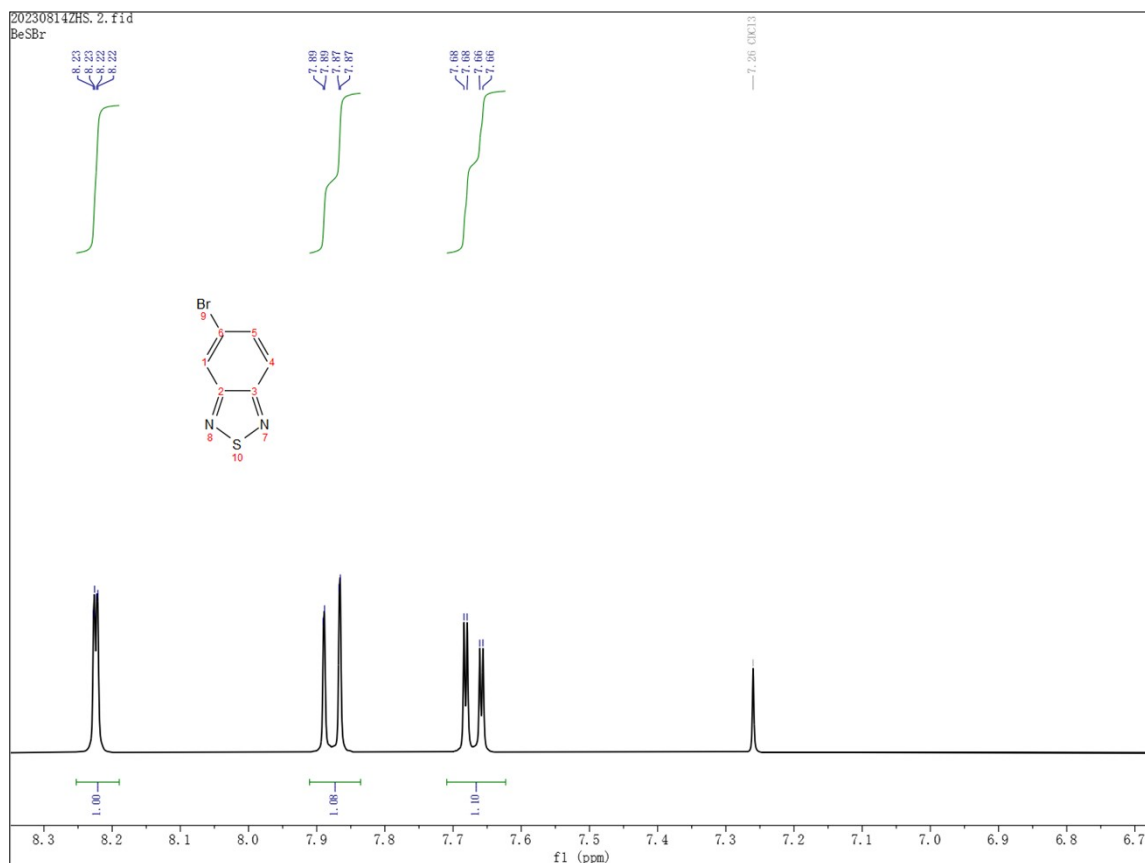


Figure S3. $^1\text{H-NMR}$ spectrum of PhS-Br in Chloroform-d.

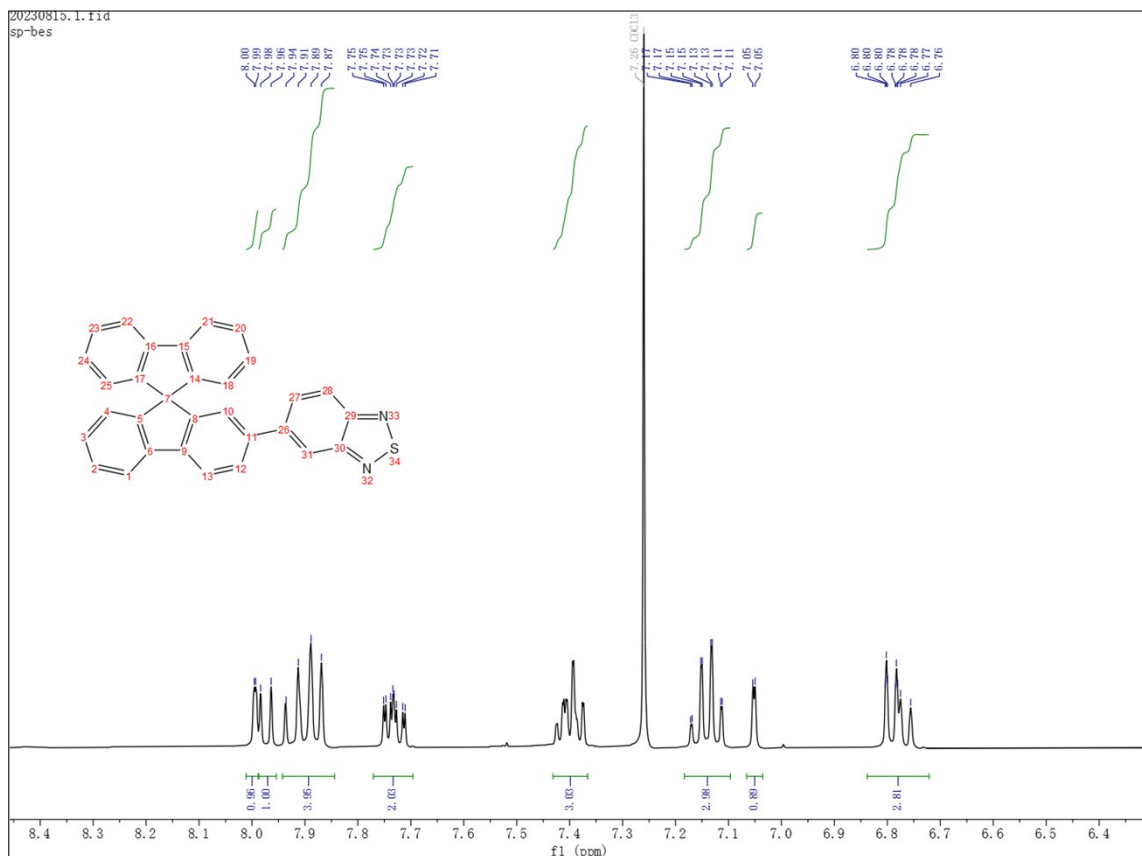


Figure S4. $^1\text{H-NMR}$ spectrum of PhS-SP in chloroform-d.

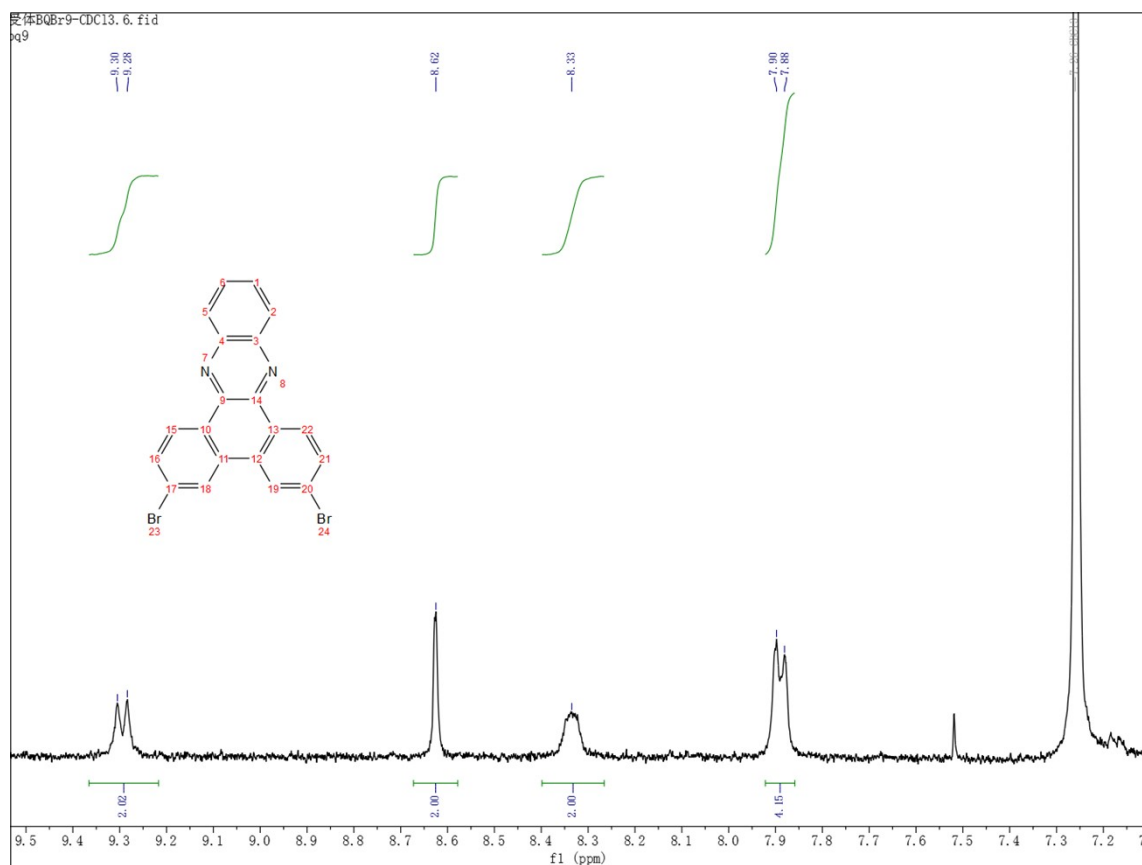


Figure S5. ¹H-NMR spectrum of DQ-Br in Chloroform-d.

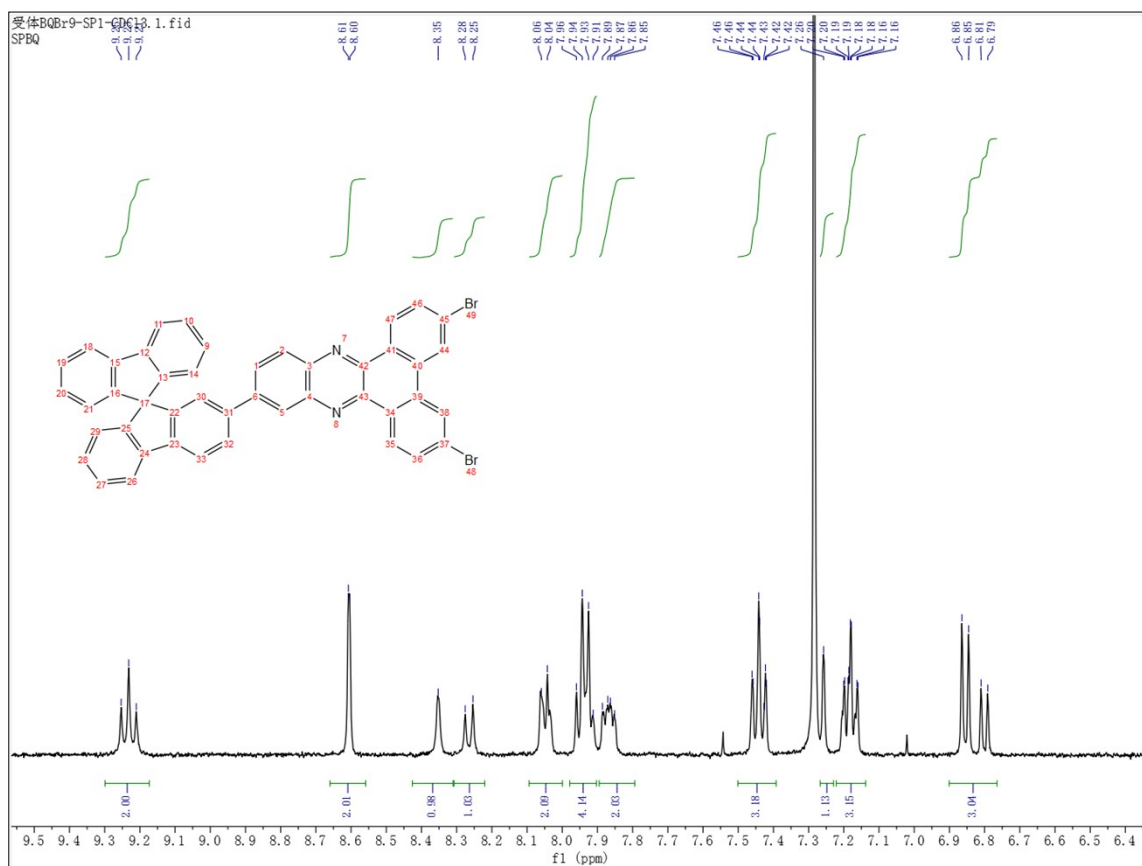


Figure S6. ¹H-NMR spectrum of DQBr-SP in Chloroform-d.

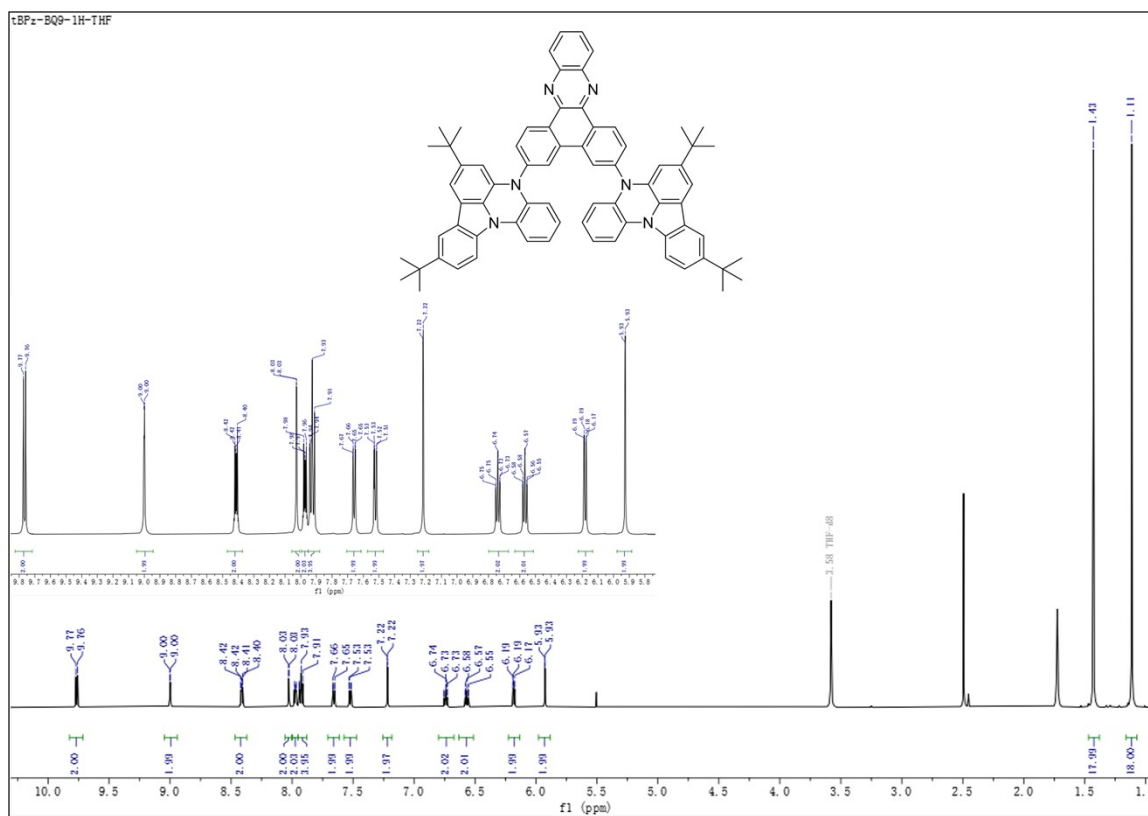


Figure S7. ¹H-NMR spectrum of tBuInPz-DQ in tetrahydrofuran-d.

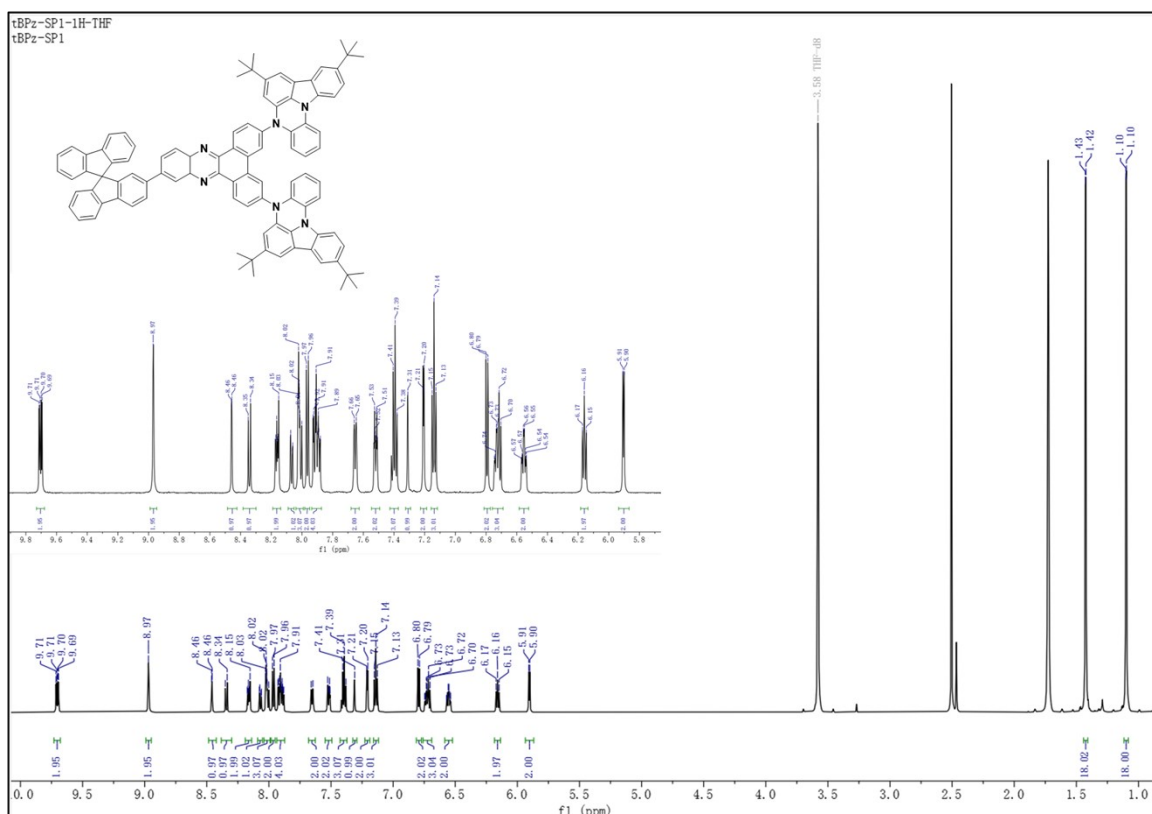


Figure S8. ^1H -NMR spectrum of tBuInPz-SP in tetrahydrofuran-d.

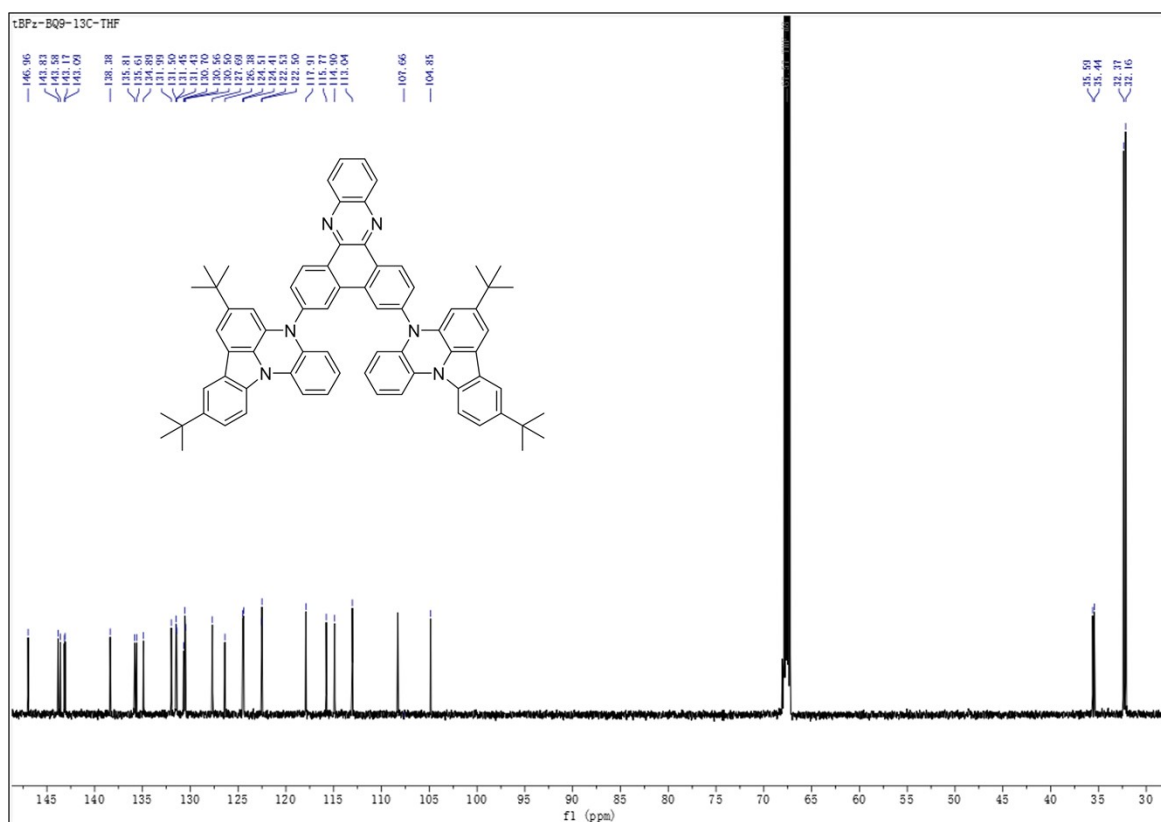


Figure S9. ^{13}C -NMR spectrum of tBuInPz-DQ in tetrahydrofuran-d.

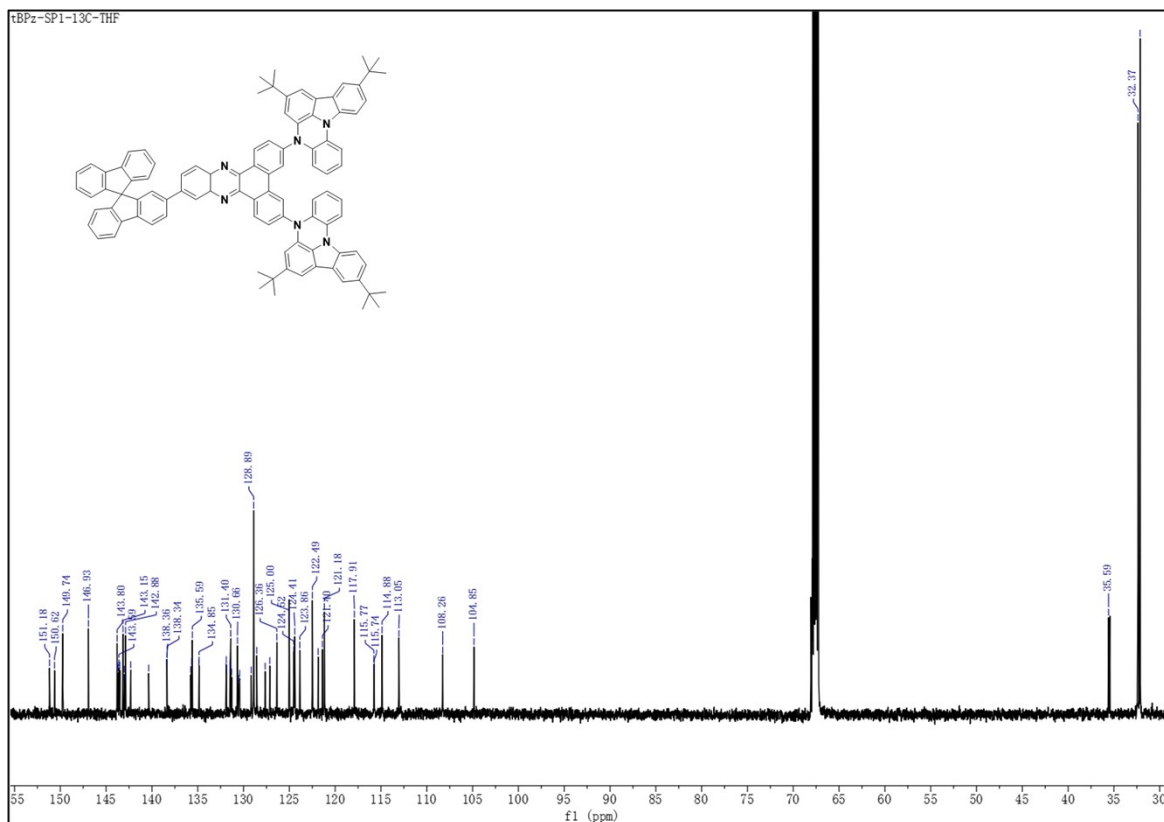


Figure S10. ^{13}C -NMR spectrum of tBuInPz-SP in tetrahydrofuran-d.

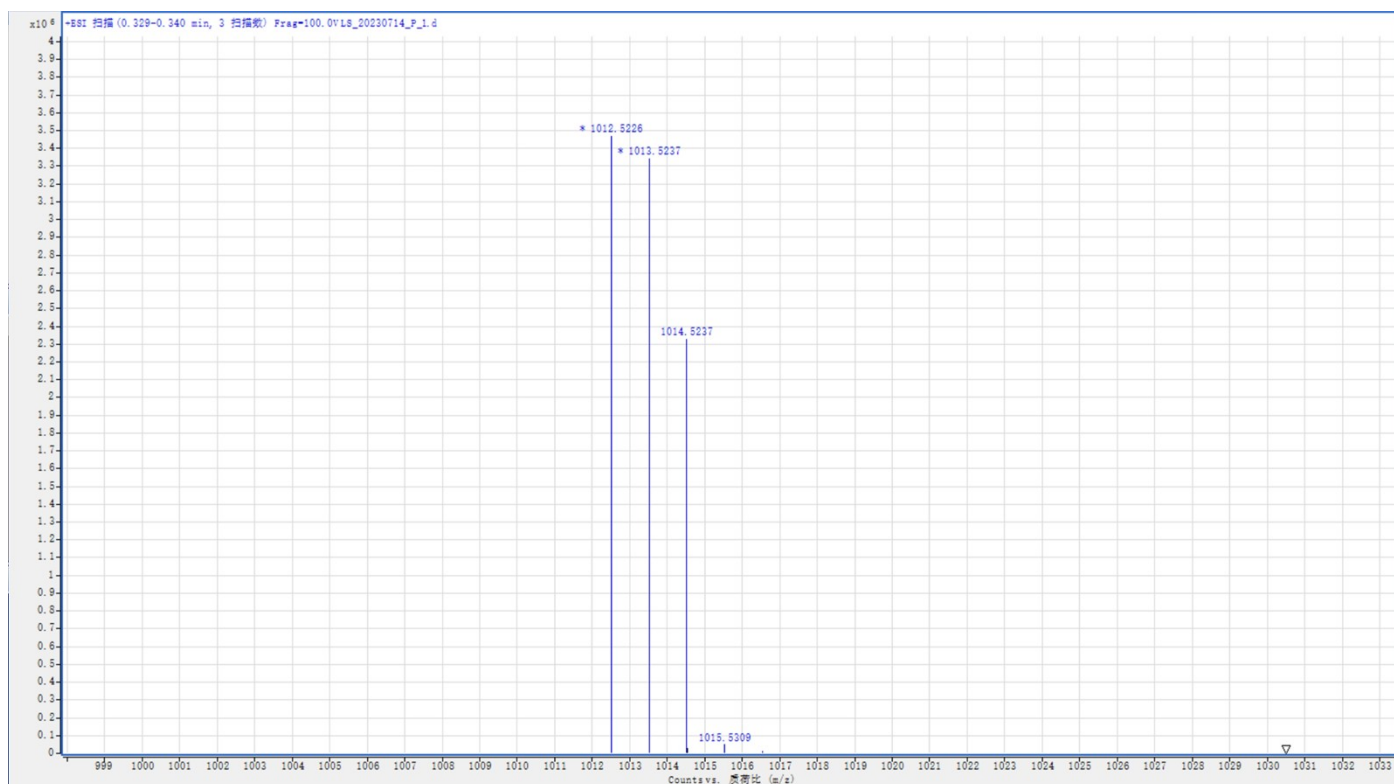


Figure S11. High-resolution mass spectra of tBulnPz-DQ.

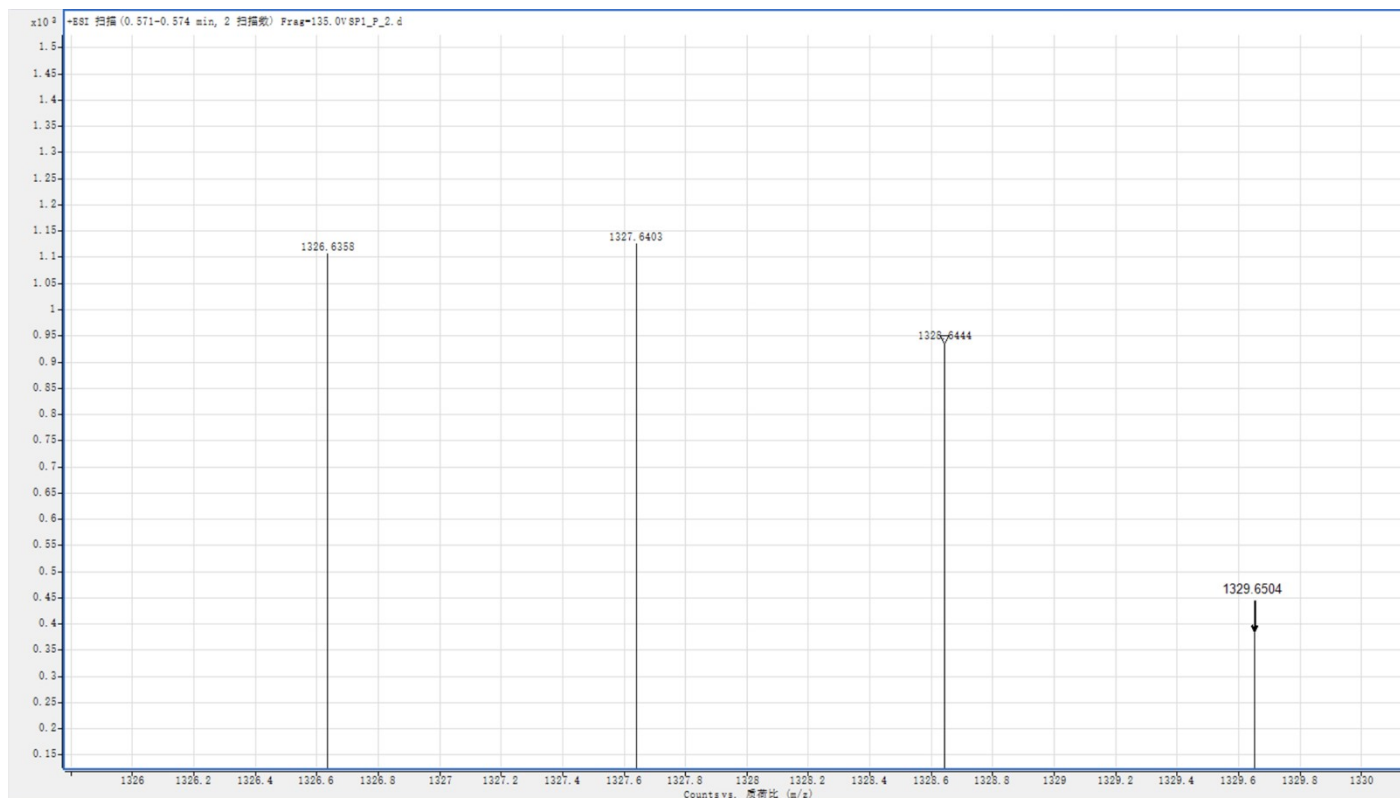


Figure S12. High-resolution mass spectra of tBuInPz-SP.

Supplementary Note 4: Supplementary figures

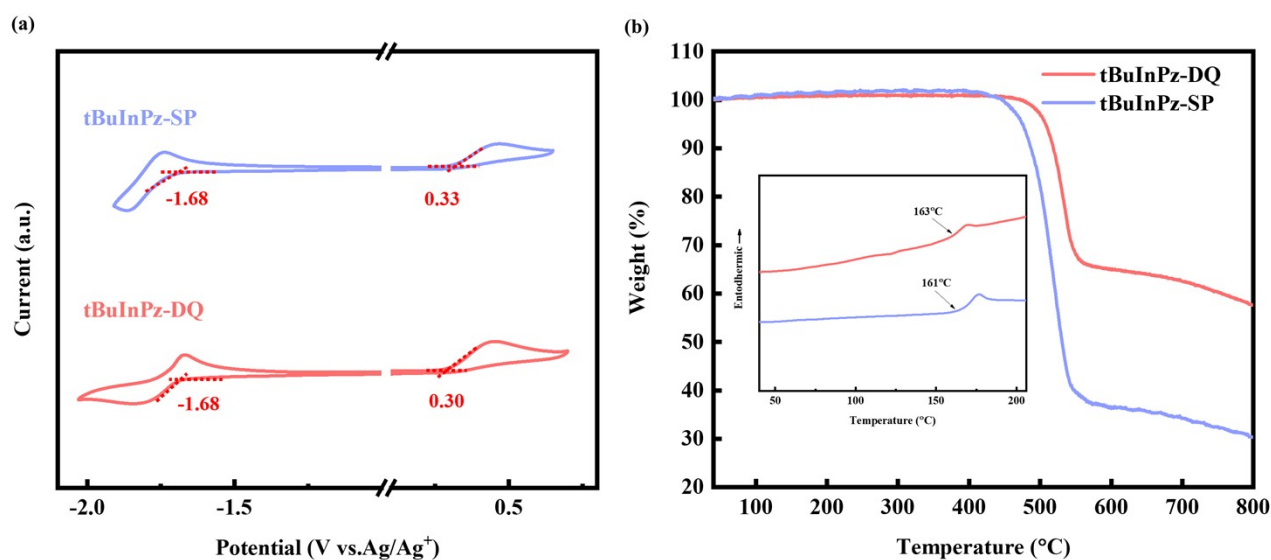


Figure S13. (a) Cyclic voltammograms: the oxidation experiments measured in dichloromethane solution. (b) TGA and DSC traces of the compounds recorded at a heating rate of $10\text{ }^{\circ}\text{C min}^{-1}$.

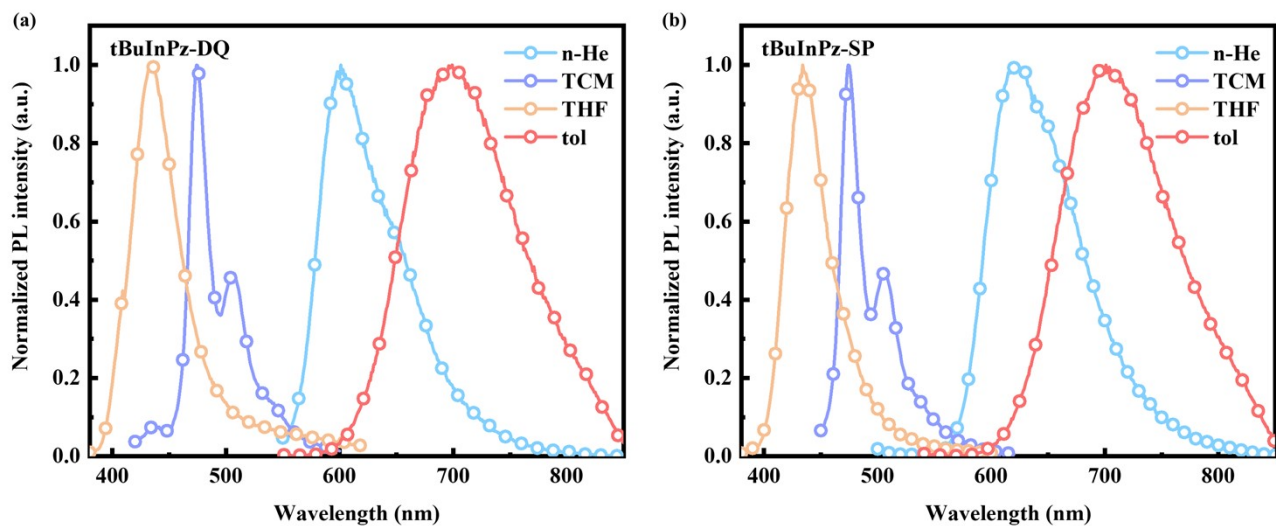


Figure S14. The PL spectra of the emitters in different solvents. (a) tBuInPz-DQ, (b) tBuInPz-SP.

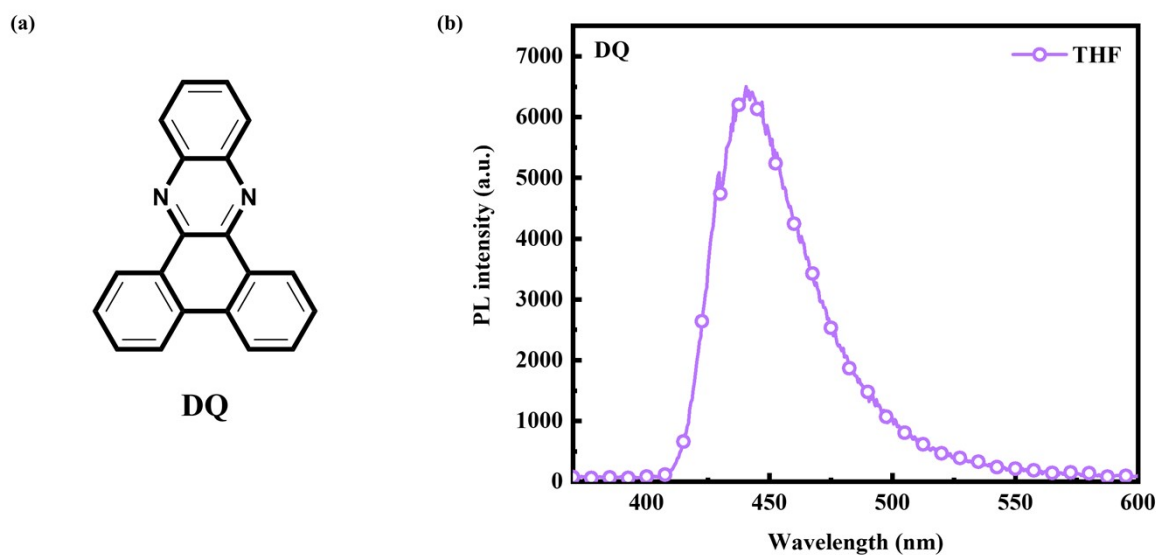


Figure S15. (a) Chemical structure of the acceptor DQ. (b) The PL spectrum of DQ in tetrahydrofuran.

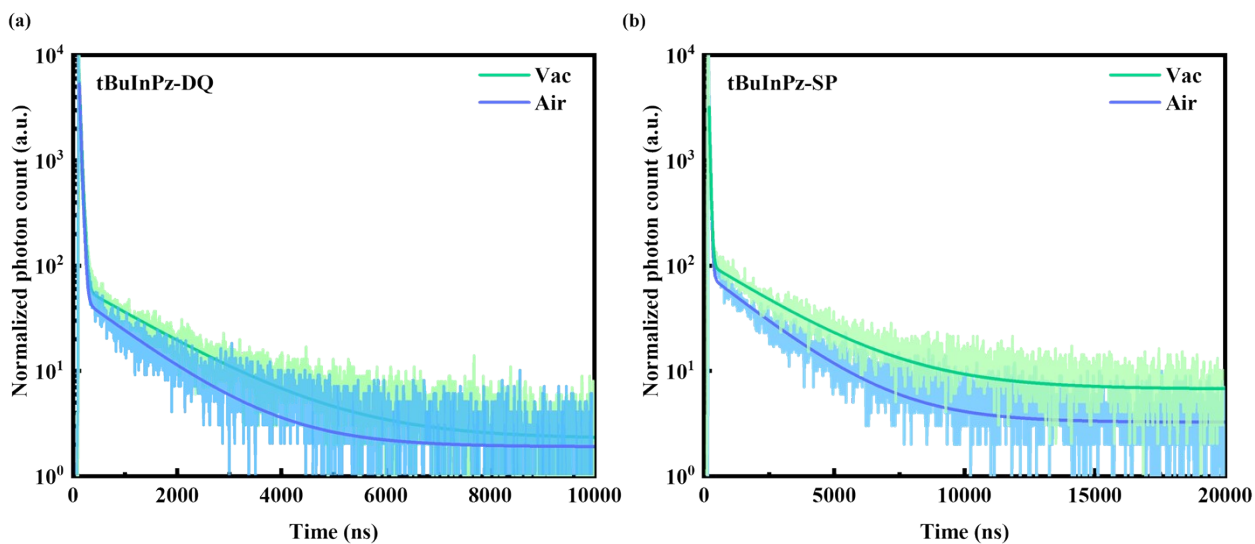


Figure S16. Transient PL spectra in air and vacuum of 1 wt% tBuInPz-DQ and tBuInPz-SP doped into TCTA host with 5 wt% PVK, respectively.

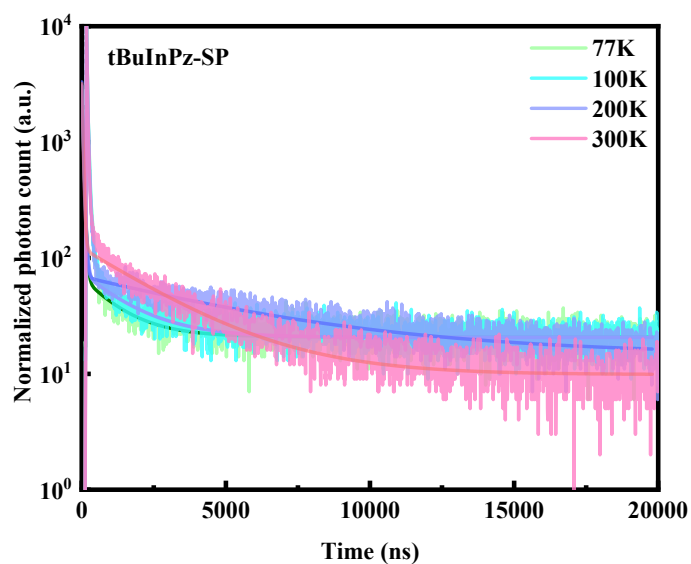


Figure S17. The temperature-dependent transient PL spectra of 1 wt% tBuInPz-SP doped into TCTA host with 5 wt% PVK.

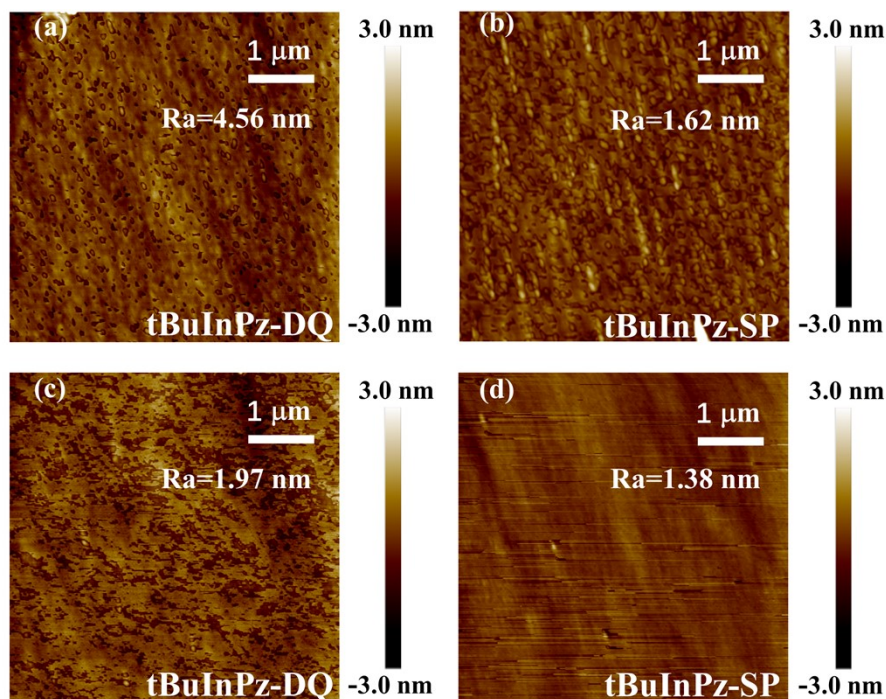


Figure S18. The height images of the films detected by atomic force microscopy: the pure film of tBuInPz-DQ (a) and tBuInPz-SP (b), the doped film of 3 wt% of tBuInPz-DQ doped into TCTA host with 5 wt% PVK (c) and the doped film of 5 wt% of tBuInPz-SP doped into TCTA host with 5 wt% PVK (d). The root mean-square surface roughness (R_a) of the whole scanning area is shown in the images.

Supplementary References

1. Y. Tao, K. Yuan, T. Chen, P. Xu, H. H. Li, R. F. Chen, C. Zheng, L. Zhang and W. Huang. *Adv. Mater.*, 2014, 26, 7931-7958.
2. Y. C. Liu, L. Hua, Z. N. Zhao, S. A. Ying, Z. J. Ren and S. K. Yan. *Adv. Sci.*, 2021, 8, 2101326.
3. P. Makuła, M. Pacia and W. Macyk. *J. Phys. Chem. Lett.*, 2018, 9, 23, 6814–6817
4. T. Lu and F. W. Chen. *J. Comput. Chem.*, 2012, 33, 580-592.
5. T. Lu and F. W. Chen. *Acta Chim. Sini.*, 2011, 69, 2393-2406.
6. W. Yang, W. M. Ning, H. Jungchi, T. X. Liu, X. J. Yin, C. Q. Ye, S. L. Gong and C. L. Yang, *Chem. Eng. J.*, 2022, 438, 135571.